NUCL SCI TECH (2018) 29:159
https://doi.org/10.1007/s41365-018-0502-1

Constraining the colored $c\bar{c}$ energy loss from J/ψ production in p-A collisions

Li-Hua Song[1] · Lin-Wan Yan[1] · Ying Liu[1]

Received: 22 June 2018 / Revised: 20 August 2018 / Accepted: 24 August 2018 / Published online: 27 September 2018

Abstract Considering the volatility of the propagation path for charmonium passing across the nuclear target in J/ψ formation from p-A collisions, the charmonium energy loss is investigated using Salgado–Wiedemann quenching weights. A successful description regarding J/ψ suppression of $R_{\mathrm{W(Fe)/Be}}(x_{\mathrm{F}})$ from the E866 experiment for $0.2 < x_{\mathrm{F}} < 0.65$ gives the transport coefficient $\hat{q} = 0.29 \pm 0.07\,\mathrm{GeV}^2/\mathrm{fm}$ for the colored $c\bar{c}$ energy loss. The calculated result indicates that radiative energy loss of a parton should be independent of its mass at high energy. The calculations are further compared to LHC and RHIC measurements.

Keywords J/ψ production · Energy loss · Charm quark · Gluon

1 Introduction

A wide range of phenomena observed from experiments on ultra-relativistic heavy-ion collisions suggests that the Quark–Gluon Plasma (QGP) has been founded [1, 2]. The suppression of J/ψ production as a result of Debye screening about heavy-quark potential at a finite temperature is a striking observable phenomenon from heavy-ion collisions which was expected as the signature of QGP formation [3, 4]. However, there are several other effects that can suppress the J/ψ yields from heavy-ion collisions for high energy [5, 6]. Among them, the energy loss effect from the particles when they go through a medium and experience collisions and eradiating gluons have received much attention. For quantifying of the properties of the QGP, it is necessary to constrain the values about the transport characteristic parameters for the cold nuclear medium by means of J/ψ formation from p-A collisions.

It is generally recognized that the process of J/ψ production from proton–nucleus collisions can be separated into three stages. As discussed in Ref. [7], the first is the perturbative (gluon fusion) production stage which leads to a colored $c\bar{c}$ pair, which is followed by the emission or absorption of a further gluon, thereby inducing color neutrality and establishing the quarkonia produced as color singlets. In the final step, the nascent J/ψ evolves into a fully grown physical charmonium resonance. The nuclear effects responsible for the suppression of J/ψ formation generally contain the modifications of the nuclear parton densities, the energy loss experienced by the incoming proton or colored $c\bar{c}$ pair when they traverse the nuclear medium, and the nuclear absorption about a $c\bar{c}$ pair or resonances. Experiments involving a wide collision energy range from NA3 [8], E772 [9], E866 [10, 11], NA50 [12], HEAR-B [13], LHC [14, 15] and RHIC [16] have revealed the drastic nuclear suppression effects.

The conventional nuclear suppression mechanism is still an open question because of the existence of many competitive effects. There are several phenomenological models proposed separately on the basis of the nuclear absorption effect of the $c\bar{c}$ pair [17, 18], the parton energy loss induced by parton multiple scattering in a nuclear

This work was supported in part by the National Natural Science Foundation of China (No. 11405043) and the Natural Science Foundation of Hebei Province (No. A2018209269).

✉ Li-Hua Song
songlh@ncst.edu.cn

[1] College of Science, North China University of Science and Technology, Tangshan 063210, China

medium [19–21], and a decrease in the overlap with the J/ψ wave function caused by the increase in the invariant mass for the $c\bar{c}$ pair with multiple soft rescatterings when they traverse the nucleus [22]. It is generally recognized that when J/ψ formation occurs outside of the nuclear target, the $c\bar{c}$ will maintain color for the entire path in the target nucleus. In this case, the color octet $c\bar{c}$ loses energy due to the medium-induced gluon radiation when traversing the target nucleus. This induces a suppression of J/ψ formation.

It was determined from our previous work that the associated medium-induced energy loss is the main effect which leads to the J/ψ suppression for J/ψ formation which occurs outside the nuclear target [20, 21]. In this investigation, our aim is to extract the transport coefficient for charm quarks by fitting the acquired experimental data to J/ψ hadronization which arises outside the nucleus. The main improvements over previous works are twofold: Using Salgado–Wiedemann (SW) quenching weights [23], our calculations include the probability that a charmonium can radiate an additional energy fraction ε in a cold nuclear medium due to scattering. In addition, we consider the volatility of the propagation path L of the charmonium passing across the nuclear target by averaging over the nuclear geometry. In view of the deviation between the modification of the parton distribution functions of the different sets, we consider the uncertainty that our calculated results originate from the nuclear parton densities by analyzing the uncertainties of the nuclear parton distribution functions.

We organized this report as follows: In Sect. 2, we will emphasize the introduction of the method adopted in this work for calculating the J/ψ formation cross section from p-A collisions modified due to the charmonium energy loss. A presentation of the results obtained and discussion is provided in Sect. 3. Finally, we will end with a brief summary in Sect. 4.

2 The modification for charmonium energy loss

As discussed in our earlier articles [20, 21], when the distance L_0 that the $c\bar{c}$ peregrinates within the appropriate color neutralization time τ_0 exceeds its passing length LA in the target nucleus, it will be colored for the whole path in the target nucleus. The $c\bar{c}$ energy loss plays the main role in J/ψ suppression for the case that J/ψ formation occurs outside the nucleus. If a color octet $c\bar{c}$ pair loses energy ε because of multiple scattering and gluon radiation, the energy loss ε will cause the rescaling of x_{F}:

$$x_{\mathrm{F}}(E) \rightarrow x'_{\mathrm{F}}(E+\varepsilon), x'_{\mathrm{F}} = x_{\mathrm{F}} + \varepsilon/E_{\mathrm{p}}. \tag{1}$$

The distribution function $D(\varepsilon)$ about the probability that a parton loses energy ε determines the nuclear modification induced by the colored $c\bar{c}$ energy loss. According to Ref. [23], if we assume that the gluon emissions are independent, the probability distribution $D(\varepsilon)$ can be expressed as:

$$D(\varepsilon) = \sum_{n=0}^{\infty} \frac{1}{n!} \left[\prod_{i=1}^{n} \int \mathrm{d}\omega_i \frac{\mathrm{d}I(\omega_i)}{\mathrm{d}\omega}]\delta(\varepsilon - \sum_{i=1}^{n} \omega_i) \exp[- \int_0^{+\infty} \mathrm{d}\omega \frac{\mathrm{d}I(\omega)}{\mathrm{d}\omega} \right], \tag{2}$$

where $\mathrm{d}I(\omega)/\mathrm{d}\omega$ represents the spectrum of the medium-induced gluon and n is the gluon number radiated by the hard parton. The probability distribution $D(\varepsilon)$ with a discrete and a continuous part is expressed as [24]:

$$D(\varepsilon) = p_0 \delta(\varepsilon) + p(\varepsilon). \tag{3}$$

Its normalization is unity.

The color evaporation model (CEM) [25] and non-relativistic QCD (NRQCD) are two successful formalisms [26] with incorporate the features of the process for J/ψ formation. Due to the formalism about NRQCD including more free parameters than CEM [27–31], we express the cross section about J/ψ formation from p-A collisions based on the CEM formalism. With the probability $\rho_{J/\psi}$ of a $c\bar{c}$ pair developing into a J/ψ state and the parton densities $f_i(x_1, m^2)$ ($f'_i(x_2, m^2)$) in proton (nucleon), $\mathrm{d}\sigma_{\mathrm{p-A}}/\mathrm{d}x_{\mathrm{F}}$ can be written as [32]:

$$\begin{aligned} \frac{\mathrm{d}\sigma_{\mathrm{p-A}}}{\mathrm{d}x_{\mathrm{F}}}(x_{\mathrm{F}}) = \rho_{J/\psi} \int_{2m_{\mathrm{c}}}^{2m_{\mathrm{D}}} \mathrm{d}m \frac{2m}{\sqrt{x_{\mathrm{F}}^2 s + 4m^2}} \\ \times [f_{\mathrm{g}}(x_1, m^2) f'_{\mathrm{g}}(x_2, m^2) \sigma_{\mathrm{gg}}(m_{\mathrm{c}}^2) \\ + \sum_{q=u,d,s} \{f_q(x_1, m^2) f'_{\bar{q}}(x_2, m^2) \\ + f_{\bar{q}}(x_1, m^2) f'_q(x_2, m^2)\} \sigma_{q\bar{q}}(m_{\mathrm{c}}^2)]. \end{aligned} \tag{4}$$

As expressed in Ref. [20, 21], the leading order cross section about the $c\bar{c}$ partonic production formed by the amalgamation of gluons or the annihilation of quark–antiquark is, respectively, σ_{gg} or $\sigma_{q\bar{q}}$.

Considering the modification due to $c\bar{c}$ energy loss with the probability $D(\varepsilon)$, the J/ψ formation cross section thus becomes

$$\frac{\mathrm{d}\sigma'_{\mathrm{p-A}}}{\mathrm{d}x_{\mathrm{F}}}(x_{\mathrm{F}}) = \int_0^{\varepsilon_{\max}} \mathrm{d}\varepsilon D(\varepsilon) \frac{\mathrm{d}\sigma_{\mathrm{p-A}}}{\mathrm{d}x_{\mathrm{F}}}(x'_{\mathrm{F}}). \tag{5}$$

In the previous formula, $x'_{1,2} = \frac{1}{2}[\sqrt{x_{\mathrm{F}}'^2(1-\tau)^2 + 4\tau} \pm x'_{\mathrm{F}}(1-\tau)]$ $(\tau = m^2/s)$ takes place $x_{1,2}$ in Eq. 4, respectively. In our calculations, the integral over ε is bounded by $\varepsilon_{\max} = \min(E_{\mathrm{p}} - E, E)$, and we use the SW quenching weights for the probability distribution $D(\varepsilon)$, which are obtained based on multiple soft and single hard scattering approximations and available as a FORTRAN routine [33].

The SW quenching weight returns results for a quark with m / E traversing a medium with transport coefficient $\hat{q}$ (it determines the transport properties of the so-called cold nuclear matter) and length L. In view of the fluctuations of the path length L traveled by the $c\bar{c}$ through the target nucleus, we consider the geometry of J/ψ formation in this process. As displayed in Fig. 1, we suppose that the target nucleus is located at $(\vec{0}, 0)$, and at $(\vec{b}, y)$ the $c\bar{c}$ pair is formed. Thus, the path length L that the $c\bar{c}$ pair propagates along in accordance with the direction of the impact parameter $\vec{b}$ can be expressed as $L = \sqrt{R_{\mathrm{A}}^2 - b^2} - y$ ($R_{\mathrm{A}} = 1.12A^{1/3}$, where y represents the coordinate along direction of the $c\bar{c}$.) [34]. It is worth mentioning that the collisions of the nucleons are not polarized, and do not rely on the direction. As such, the expression of the path length L does not depend on the direction of the $c\bar{c}$ pair. The J/ψ formation cross section $\mathrm{d}\sigma''_{\mathrm{p-A}}/\mathrm{d}x_{\mathrm{F}}$ which contains the modification of the nuclear geometry effect, can be expressed as:

$$\frac{\mathrm{d}\sigma''_{\mathrm{p-A}}}{\mathrm{d}x_{\mathrm{F}}}(x_{\mathrm{F}}) = \int \mathrm{d}^2b\mathrm{d}y\rho_{\mathrm{A}}(\overrightarrow{b}, y)\frac{\mathrm{d}\sigma'_{\mathrm{p-A}}}{\mathrm{d}x_{\mathrm{F}}}(x_{\mathrm{F}}). \tag{6}$$

In the preceding formula, the y is from $-\sqrt{R_{\mathrm{A}}^2 - b^2}$ to $\sqrt{R_{\mathrm{A}}^2 - b^2}$, and the nuclear density distribution $\rho_{\mathrm{A}}(\vec{b}, y)$ is normalized to unity $(\rho_{\mathrm{A}}(\sqrt{b^2 + y^2}) = (\rho_0/A)\Theta(R_{\mathrm{A}} - \sqrt{b^2 + y^2}))$ [35–37].

The effect of the incident proton can decrease the center-mass system energy of the nucleon-–nucleon collision for producing the $c\bar{c}$. As such, the momentum fraction becomes x_{F} rescaled again [38]:

$$x''_{\mathrm{F}} = r_{\mathrm{s}}x'_{\mathrm{F}} = r_{\mathrm{s}}(x_{\mathrm{F}} + \varepsilon/E_{\mathrm{p}}), \tag{7}$$

with $r_{\mathrm{s}} = \sqrt{s}/\sqrt{s'}$, $\sqrt{s'} = \sqrt{s} - (n-1)\triangle\sqrt{s}$, and n denoting the number of collisions for the incident proton with the nucleons in the nuclear target. Based on the Glauber model [39], the J/ψ formation cross section for p-A collisions is ultimately:

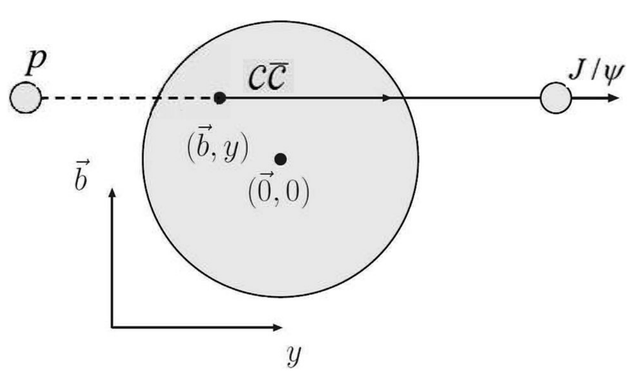

Fig. 1 Demonstration of the geometry of J/ψ formation from p-A collisions

$$\left\langle \frac{\mathrm{d}\sigma_{\mathrm{p-A}}}{\mathrm{d}x_{\mathrm{F}}} \right\rangle = \sum_{n=1}^{A} P(n)\frac{\mathrm{d}\sigma^{(n)}_{\mathrm{p-A}}}{\mathrm{d}x_{\mathrm{F}}}(x_{\mathrm{F}}). \tag{8}$$

In the preceding formula, $\frac{\mathrm{d}\sigma^{(n)}_{\mathrm{p-A}}}{\mathrm{d}x_{\mathrm{F}}}(x_{\mathrm{F}}) = \frac{\mathrm{d}\sigma''_{\mathrm{p-A}}}{\mathrm{d}x_{\mathrm{F}}}(x''_{\mathrm{F}})$ denotes the J/ψ production cross section in the nth collision, and the probability $P(n)$ of the projectile proton scattering inelastically on the nuclear target for possessing n collisions with nucleons is given as:

$$P(n) = \frac{\int \mathrm{d}\vec{b}P(n, \vec{b})}{\sum_{n=1}^{A}\int \mathrm{d}\vec{b}P(n, \vec{b})}, \tag{9}$$

with $P(n, \vec{b}) = \frac{A!}{n!(A-n)!}[T(\vec{b})\sigma_{\mathrm{in}}]^n[1 - T(\vec{b})\sigma_{\mathrm{in}}]^{A-n}$. According to Ref. [40], for $A \leq 32$ the thickness function $T(\vec{b}) = \frac{1}{2\pi\beta_{\mathrm{A}}^2}\exp(-\vec{b}^2/2\beta_{\mathrm{A}}^2)$, $T(\vec{b}) = \frac{3}{2\pi R_{\mathrm{A}}^3}\sqrt{R_{\mathrm{A}}^2 - \vec{b}^2}\theta(R_{\mathrm{A}} - |\vec{b}|)$ for $A > 32$. See details in Ref. [20, 21].

3 Results and discussion

In order to facilitate the theoretical investigation of the parton energy loss in cold nuclear matter, the extraction of the value of the transport coefficient $\hat{q}$ about the charmonium energy loss by means of J/ψ formation experimental data is necessary. The transport coefficient $\hat{q}$ determines the amount about the medium-induced gluon radiation and the J/ψ suppression strength. In view of Ref. [41], if an appropriate color neutralization time $\tau_0 = 0.25$ fm is assumed, then $L_0 > L_{\mathrm{A}}$ for $x_{\mathrm{F}} > 0$ with $\sqrt{s} = 40$ GeV. This indicates that the $c\bar{c}$ will be colored along its entire path at E866 energy for $x_{\mathrm{F}} > 0$. Therefore, the E866 experimental data for J/ψ production provide a reliable approach for investigating the colored $c\bar{c}$ energy loss. To constrain the transport coefficient $\hat{q}$ about the colored $c\bar{c}$ energy loss, we perform the calculation about the J/ψ formation cross-sectional ratios $R_{\mathrm{W(Fe)/Be}}(x_{\mathrm{F}})$:

$$R_{\mathrm{W(Fe)/Be}}(x_{\mathrm{F}}) = \left\langle \frac{\mathrm{d}\sigma_{\mathrm{p-W(Fe)}}}{\mathrm{d}x_{\mathrm{F}}} \right\rangle \Big/ \left\langle \frac{\mathrm{d}\sigma_{\mathrm{p-Be}}}{\mathrm{d}x_{\mathrm{F}}} \right\rangle \tag{10}$$

at E866 energy.

Using the CERN subroutine MINUIT [42], based on the minimization of the function of χ^2, the transport coefficient $\hat{q}$ for $c\bar{c}$ energy loss is extracted. Table 1 shows the values of the transport coefficient $\hat{q}$ and corresponding χ^2/ndf obtained from the data of the E866 experiment on J/ψ production in different x_{F} intervals. With an increase in χ^2 by 1 unit from its minimum χ^2_{min}, we allow one standard deviation of the parameter from the central fit. In our calculation, the SW quenching weights [23] were used to describe the probability distribution for $c\bar{c}$ energy loss, and

Table 1 $\hat{q}$ for $c\bar{c}$ energy loss and χ^2/ndf constrained by fitting E866 data on $R_{\mathrm{W(Fe)/Be}}(x_{\mathrm{F}})$

x_{F}	No.data	$\hat{q}$ (GeV^2/fm)	χ^2/ndf
$0.20 < x_{\mathrm{F}} < 0.65$	18	0.29 ± 0.07	0.73
$0.30 < x_{\mathrm{F}} < 0.95$	26	0.31 ± 0.05	10.80
$0.20 < x_{\mathrm{F}} < 0.95$	44	0.29 ± 0.05	7.21

utilize EPS09 nuclear parton densities [43] and CTEQ6L proton parton distributions [44], and $\triangle\sqrt{s} = 0.18$GeV which originates in the energy loss of the incident proton [45].

From Table 1, we can see that the theoretical results for the middle x_{F} region ($0.2 < x_{\mathrm{F}} < 0.65$) agree well with the data for $\hat{q} = 0.29 \pm 0.07\,\mathrm{GeV}^2$/fm and the corresponding $\chi^2/ndf = 0.73$, and for the region including the large x_{F} ($0.3 < x_{\mathrm{F}} < 0.95$) the calculated results greatly deviate from the experimental data ($\hat{q} = 0.31 \pm 0.05\,\mathrm{GeV}^2$/fm, $\chi^2 = 10.80$). The reason may be that nuclear absorption effect plays a role in the suppression of J/ψ formation for large x_{F} region, which hinders the exact constraint of the transport coefficient $\hat{q}$. This provides the insight that we should use the experimental data for the middle x_{F} region to constrain the massive parton energy loss from the J/ψ formation. Then, $\hat{q} = 0.29 \pm 0.07\,\mathrm{GeV}^2$/fm is the determined value. By comparing with the value $\hat{q} = 0.32 \pm 0.04\,\mathrm{GeV}^2$/fm obtained from the nuclear Drell–Yan data with SW quenching weights [46], we find that these two values are nearly equal. This indicates that the radiative energy loss of a parton should become independent of its mass at high energy, as discussed in Armesto et al. [47] and in the earlier Dokshitzer-Kharzeev article [48].

In addition, the origin of the uncertainty with respect to our calculated results may originate from the uncertainty of the nuclear parton distribution functions especially for the nuclear modification of gluon densities. Recently, the K. J. Eskola et al. group proposed a new set of nuclear parton distribution functions EPPS16 [49], which initially imposed constraints on the experimental data from LHC proton–lead collisions and provided the uncertainty estimates from the central fit for each flavor. The comparison of the calculated results $R_{\mathrm{W(Fe)/Be}}(x_{\mathrm{F}})$ modified only by the nuclear effects of the parton distribution functions from the EPPS16 (dashed lines) and EPS09 (solid lines) are shown in Fig. 2. It is found that for E866 energy ($\sqrt{s} = 38.79$ GeV)the difference between the results obtained using the EPPS16 and EPS09 is very small. Moreover, for RHIC energy ($\sqrt{s} = 200.0$ GeV), the difference is slightly obvious in the region $y < -1.5$, and for LHC energy ($\sqrt{s} = 5.0$ TeV) the difference becomes increasingly obvious with the increase in y in the range $y > 0$. From Fig. 2, we also can see that the tendency of the solid and dashed lines are almost identical with the increase in x_{F} or y. By means of the EPPS16 nuclear parton distribution functions, the transport coefficient $\hat{q}$ for the colored $c\bar{c}$ energy loss extracted from the E866 experimental data in the middle x_{F} region ($0.20 < x_{\mathrm{F}} < 0.65$) is also $\hat{q} = 0.29 \pm 0.05\,\mathrm{GeV}^2$/fm (according to the central fit of EPPS16). The errors of $\hat{q}$ which originate from the uncertainty of EPPS16 are analyzed: $\hat{q} = 0.33 \pm 0.04$ GeV^2/fm according to the EPPS16 error sets S_1^- and $\hat{q} = 0.26 \pm 0.05\,\mathrm{GeV}^2$/fm according to error sets S_1^+.

To intuitively display the charmonium energy loss effect on the J/ψ formation cross-sectional ratio in p-A collisions by means of the values of the transport coefficient $\hat{q}$ shown in Table 1, our numeric results are compared with the corresponding E866 experimental data in Fig. 3 ($0.20 < x_{\mathrm{F}} < 0.65$) and Fig. 4 ($0.30 < x_{\mathrm{F}} < 0.95$). The J/ψ predictions displayed by the solid curves are obtained with the consideration of the nuclear effects of parton distributions and the energy loss effects of the incident proton and the color octet $c\bar{c}$. The tendency of the solid lines in Figs. 3 and 4 indicates that the theoretical results associated with the charmonium energy loss effect agree well with the experimental data. This implies that the effect of the $c\bar{c}$ energy loss mainly contributes to the J/ψ suppression for hadronization occurring outside the nucleus.

In order to constrain the influence of the $c\bar{c}$ energy loss on $R_{\mathrm{W(Fe)/Be}}(x_{\mathrm{F}})$, in Figs. 3 and 4 we provide the dashed lines which correspond only to the calculations with the nuclear effects on the parton distribution functions and the energy loss of the proton beam. In Fig. 3, the comparison between the J/ψ predictions with (solid line) and without (dashed line) $c\bar{c}$ energy loss shows that the strength of the J/ψ suppression in p-W (p-Fe) collisions induced by $c\bar{c}$ energy loss is approximately equal in the range $0.20 < x_{\mathrm{F}} < 0.65$. Nevertheless, in Fig. 4, the comparison between the trend of the solid and dashed lines displays that the nuclear suppression on $R_{\mathrm{W/Be}}(x_{\mathrm{F}})$ and $R_{\mathrm{Fe/Be}}(x_{\mathrm{F}})$ due to $c\bar{c}$ energy loss decreases gradually with the increase in x_{F} in the range $0.65 < x_{\mathrm{F}} < 0.80$ and further reduces slowly in $x_{\mathrm{F}} > 0.80$. For Fig. 3, from the gap between the solid and dashed lines, we can also determine that the suppression strength for $R_{\mathrm{W/Be}}(x_{\mathrm{F}})$ is about 10%, which is larger than that (approximately 5%) of $R_{\mathrm{Fe/Be}}(x_{\mathrm{F}})$. The comparison between the J/ψ predictions as indicated by the solid line for $R_{\mathrm{W/Be}}(x_{\mathrm{F}})$ and that for $R_{\mathrm{Fe/Be}}(x_{\mathrm{F}})$ reveal that the energy loss of the charmonium plays a more important role in the suppression of J/ψ cross-sectional ratios $R_{\mathrm{W/Be}}(x_{\mathrm{F}})$ than $R_{\mathrm{Fe/Be}}(x_{\mathrm{F}})$. This indicates that the effect of the color octet $c\bar{c}$ energy loss should be extremely

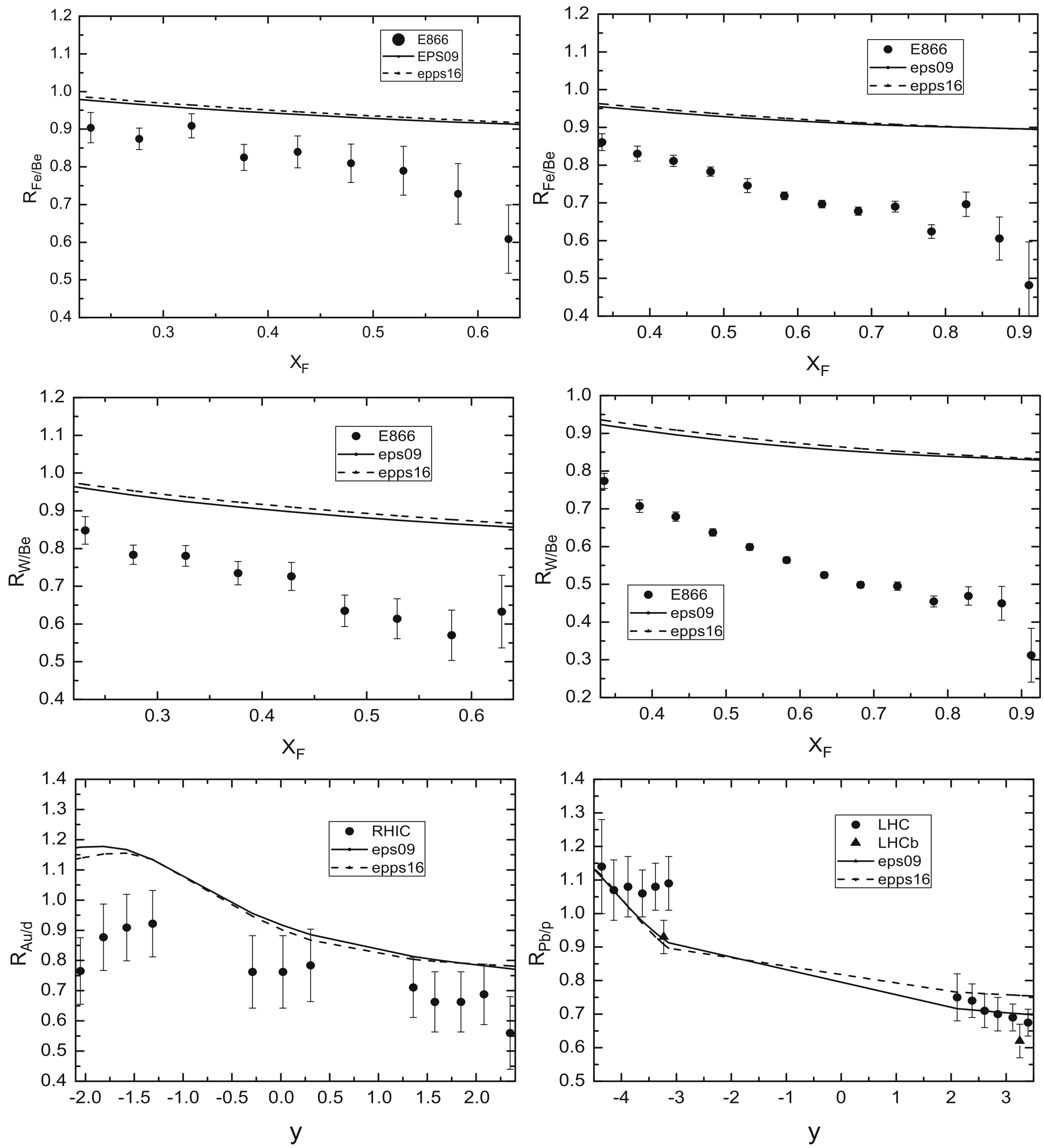

Fig. 2 A comparison of the calculated results modified only by the nuclear effects of the parton distributions from EPPS16 (dashed lines) and EPS09 (solid lines)

important for large targets. The same conclusion can be drawn from Fig. 4.

In addition, for investigating the nuclear effects of gluon distribution functions on J/ψ suppression, we describe the theoretical results with only the nuclear modification of quark distributions and energy loss of the proton beam as the dotted lines in Figs. 3 and 4. It can be seen that the difference between the dotted and dashed lines is small, especially for the range $x_F > 0.7$, which means that the nuclear effects of the gluon distributions in the nucleon have little influence on J/ψ suppression within the middle and large x_F range $(0.2 < x_F < 0.95)$ for E866 energy $(E_p = 800$ GeV).

Furthermore, with $x_F = \frac{2m}{\sqrt{s}} \sinh y$ and $E = E_p e^y m/\sqrt{s}$, J/ψ the formation cross-sectional ratios with y as a variable are calculated for RHIC ($\sqrt{s} = 200$ GeV) and LHC ($\sqrt{s} = 5.0$ TeV) experimental data. The energy loss ε of the octet $c\bar{c}$ also causes rescaling of the variable y:

$$y' = y + \ln\left(\frac{E + \varepsilon}{E}\right), \tag{11}$$

and then

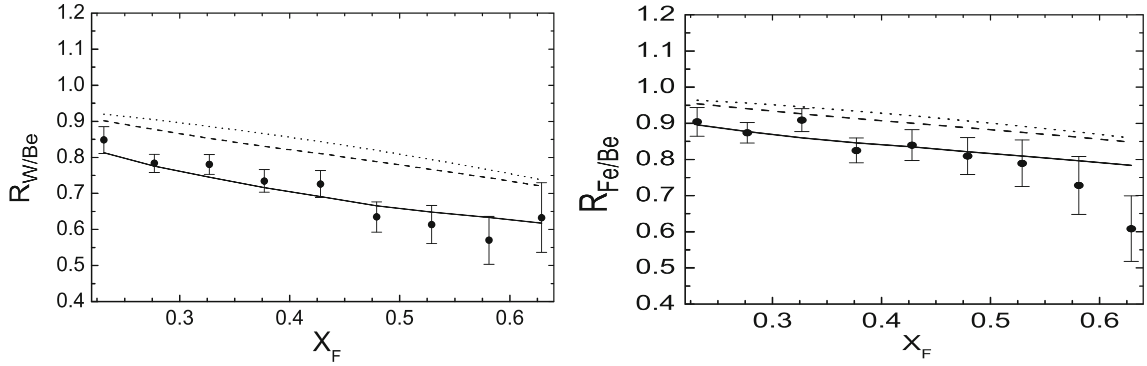

Fig. 3 E866 J/ψ suppression data for the range $0.2 < x_F < 0.65$ in p-W(Fe) collisions [10, 11] compared to the energy loss model. The theoretical results for the nuclear effects of the quark (quark and gluon) density and the incident proton energy loss effect are represented by the dotted (dashed) lines, and the solid curves represent the calculations including the two aforementioned effects and the $c\bar{c}$ energy loss effect. Error bars represent the statistical uncertainty

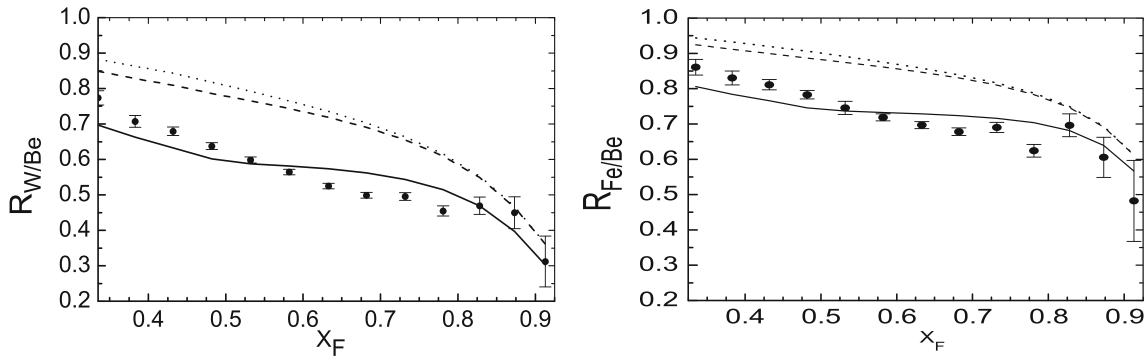

Fig. 4 E866 J/ψ suppression data for the range $0.3 < x_F < 0.95$ in p-W(Fe) collisions [10, 11] compared to the energy loss model. The other comments are the same as those in Fig. 3

$$x_1' = \frac{m}{\sqrt{s}} e^{y'}, x_2' = \frac{m}{\sqrt{s}} e^{-y'}. \tag{12}$$

Considering the nuclear geometry effect of the length that the colored $c\bar{c}$ passes through in the nuclear target and using SW quenching weights, the theoretical results $R_{\mathrm{Au/d}}(y)$ modified by this colored $c\bar{c}$ energy loss model are compared with the RHIC [16] experimental data in Fig. 5. The theoretical result obtained by the nuclear modification of the parton distribution functions and the energy loss effects of the proton beam and the color octet $c\bar{c}$ ($\hat{q} = 0.29 \pm 0.07\,\mathrm{GeV}^2/\mathrm{fm}$) is shown as the solid line. The tendency of the solid curve steeply decreases with the increase in y in the range $y < 0.5$ and decrease gradually in the range $0.5 < y < 2.4$. The dashed lines correspond to calculations only with the nuclear effects on the quark and gluon distribution functions and the energy loss of the proton beam. The drift of the dashed profile shows an obvious flat behavior in the range $y < -1.5$, and then decrease with the increase in y, which is approximately consistent with the solid line. In addition, the calculated results of $R_{\mathrm{Au/d}}(y)$ containing the modification induced by the nuclear effect of the gluon density shows an

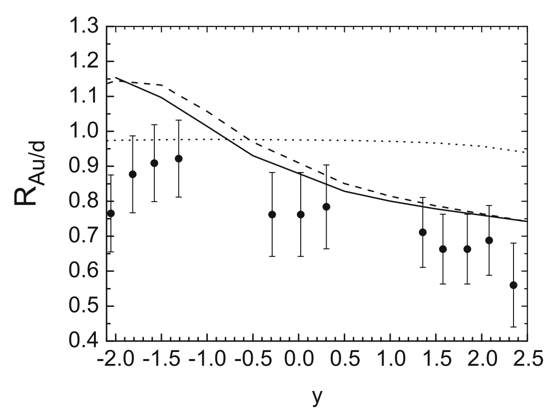

Fig. 5 J/ψ suppression data from d-Au collisions for the range $-2.2 < y < 2.4$ at RHIC [16] compared to the energy loss model. The other comments are the same as those in Fig. 3

enhancement in the range $y < -0.5$. The physical reason may be that the gluon anti-shadowing effect induces the enhancement in this coverage. From Fig. 5, we can see that there is a small gap between the solid and dashed lines and it becomes smaller with an increase in y. In addition, the two curves coincide at approximately $y > 2.0$. This means that the suppression of the J/ψ production caused by the energy loss of the colored $c\bar{c}$ is small.

Furthermore, in order to discuss the suppression induced by the nuclear modification from the gluon distributions on J/ψ production for high energy, the dotted line denotes the theoretical result with only the nuclear effects of the quark distribution functions and energy loss of proton beam is given in Fig. 5. The tendency of the dotted line is nearly flat with the increase in y in the region $-2.2<y<2.4$. The small suppression (about 3%) due to the nuclear modification of the quark distributions and energy loss of the proton beam implies that for RHIC energy, the incident proton energy loss in the initial state and the nuclear effects of the quark distribution functions have little influence on J/ψ production in the range $-2.2<y<2.4$. However, the large deviation between the dashed and dotted lines mean that the nuclear effects of gluon distributions in the nucleus play the main role in the J/ψ production at RHIC energy in the region $-2.2<y<2.4$.

In Fig. 6, we compare our calculated results based on this energy loss model with the J/ψ suppression data for the range $-4.46<y<3.53$ in p-Pb collisions from ALICE [14] (LHCb [15]) at LHC energy. The solid line indicates the theoretical result obtained by the nuclear modification of the parton distribution functions and the energy loss effects of the proton beam and the color octet $c\bar{c}$ ($\hat{q}=0.29\pm0.07$ GeV^2/fm). From Fig. 6, we can see that $R_{\mathrm{Pb/p}}(y)$ described by the solid line transitions into a trend indicating an enhancement in $y<-3.53$ and decrease with the increase in y in $-4.46<y<3.53$. The calculation with the nuclear modification on parton densities and the energy loss effect of the incoming proton is described as the dashed curve. The tendency of the dashed profile displays a high similarity with that of the solid line. There is an enhancement in the range $-4.4<y<-3.8$ both in the solid and dashed lines which contain the modification

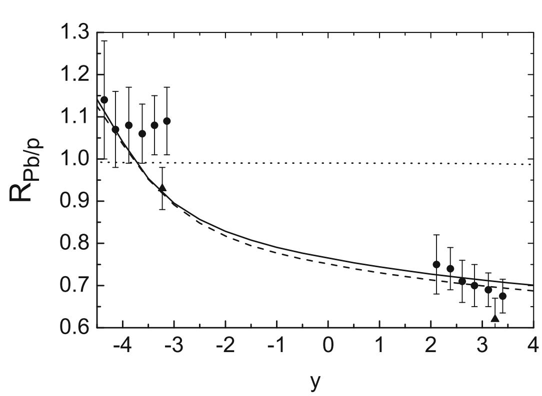

Fig. 6 J/ψ suppression data from p-Pb collisions in the range $-4.46<y<3.53$ from ALICE [14] (LHCb [15]) at LHC compared to the energy loss model. The other comments are the same as those in Fig. 3

induced by the nuclear effect of the gluon distribution functions, which would be induced by the gluon anti-shadowing effect in this coverage. In Fig. 6, it is shown that the solid and dashed curves nearly coincide at about $y<-3.0$, and there is a small gap between them in the range $y>-3.0$. Moreover, the gap is almost equal to the increase in y for $y>-3.0$. This implies that the energy loss effect of the colored $c\bar{c}$ has little influence on the suppression of the J/ψ production.

In addition, the calculated result with only the nuclear effect of the quark distribution functions and the energy loss effect of the incoming proton is displayed as the dotted line in Fig. 6. The dotted line is approximately equal to 1.0 with the increase in y in $-4.46<y<3.53$. The suppression induced by the nuclear effects of the quark distribution functions and energy loss effect of the incoming proton can be ignored (about 1%). This indicates that at the LHC energy, the incident proton energy loss in the initial state and the nuclear effects of the quark distribution functions have little influence on the calculations related to the suppression of the J/ψ production in $-4.46<y<3.53$. Nevertheless, the significant deviation from the dashed and dotted curves indicate that the nuclear modification of the gluon distribution functions in nucleon has a dominant role on the J/ψ suppression at LHC energy in the region $-4.46<y<3.53$. As displayed in Ref. [38], the nuclear modification of the gluon distribution function given by the different nuclear parton distribution sets exhibit obvious distinction. Therefore, operating precise measurements on nuclear parton distribution functions can help to exactly constrain the charmonium energy loss in cold nuclear matter at high energies such as RHIC and LHC energy.

Finally, as shown in Figs. 5 and 6, for the small kinematic coverage of LHC [14, 15] ($-7.31\times10^{-2}<x_F<7.31\times10^{-2}$) and RHIC[16]($-8.70\times10^{-2}<x_F<0.125$) experiments, the nuclear effects of gluon distributions in the nucleus play the main role on J/ψ suppression. This further supports intuitively the prediction that the gluon shadowing or gluon saturation could cause J/ψ suppression for small x_F region at high energy. For LHC and RHIC energy, the effect of the proton energy loss should be negligible since the proton energy in the nuclear rest frame is extremely large.

4 Summary

The experiment on J/ψ formation from proton–nucleus collisions provides a good environment to test the microscopic dynamics of medium-induced charmonium energy loss. Considering the volatility of the propagation path for the charmonium traversing the nuclear target, the charmonium energy loss is investigated using SW quenching weights. Based on the CERN subroutine MINUIT, by minimization of the function of χ^2, the transport coefficient $\hat{q}$ for $c\bar{c}$ energy loss is determined by fitting the data for $0.2 < x_F < 0.65$: $\hat{q} = 0.29 \pm 0.07$ GeV^2/fm with $\chi^2/ndf = 0.73$. By comparing with the value $\hat{q} = 0.32 \pm 0.04$ GeV^2/fm obtained from the nuclear Drell–Yan data with SW quenching weights, we determined that these two values are nearly equal. This indicates that radiative energy loss of a parton should become independent of its mass at high energy. In addition, in view of the deviation between the modification of the parton distribution functions of the different sets, we consider the uncertainty of our calculated results originating from the nuclear parton densities by analyzing the uncertainties of the nuclear parton distribution functions. Based on the recent EPPS16 parton distribution set, the errors of $\hat{q}$ from the uncertainty of the recent EPPS16 sets are calculated: $\hat{q} = 0.33 \pm 0.04$ GeV^2/fm according to EPPS16 error sets S_1^- and $\hat{q} = 0.26 \pm 0.05$ GeV^2/fm according to S_1^+. With the central fit of EPPS16, the value of $\hat{q}$ is extracted from the E866 experimental data for the region $0.20 < x_F < 0.65$ is still $\hat{q} = 0.29 \pm 0.05$ GeV^2/fm. By comparing with the data at RHIC and LHC, we find that for the small kinematic coverage of LHC ($-7.31 \times 10^{-2} < x_F < 7.31 \times 10^{-2}$) and RHIC($-8.70 \times 10^{-2} < x_F < 0.125$) experiment, the nuclear effects of gluon distributions in the nucleus play the main role in J/ψ suppression. In addition, due to the gigantic proton energy, the energy loss effect of proton beam has little influence. Therefore, to further exactly constrain the charmonium energy loss in cold nuclear medium, in the future, it would be desirable to perform precise measurements on J/ψ suppression from p-A collisions for middle x_F kinematic coverage.

References

1. S.S. Adler et al., (PHENIX collaboration), Suppressed π^0 production at large transverse momentum in central Au + Au collisions at $\sqrt{S_{NN}} = 200$ GeV. J. Phys. Rev. Lett. **91**, 072301 (2003). https://doi.org/10.1103/PhysRevLett.91.072301
2. J. Admodt et al., (STAR collaboration), Transverse momentum and collision energy dependence of high p(T) hadron suppression in Au + Au collisions at ultrarelativistic energies. J. Phys. Rev. Lett. **91**, 172302 (2003). https://doi.org/10.1103/PhysRevLett.91.172302
3. S. Chatrchyan et al., (CMS Collaboration), Study of high-pT charged particle suppression in PbPb compared to pp collisions at $\sqrt{S\ NN} = 2.76$ TeV. Eur. Phys. J. C **72**, 1945 (2012). https://doi.org/10.1140/epjc/s10052-012-1945-x
4. T. Matsui, H. Satz, J/ψ suppression by quark-gluon plasma formation. Phys. Lett. B **178**, 416 (1986). https://doi.org/10.1016/0370-2693(86)91404-8
5. A.D. Frawley, Heavy flavor in heavy-ion collisions at RHIC and RHIC II. J. Phys. Rep. **462**, 125 (2008). https://doi.org/10.1016/j.physrep.2008.04.002
6. H.-M. Wang, J/ψ production in p + p and p + Pb collisions at ultrarelativistic energies. J. Nucl. Sci. Technol. **29**, 116 (2018). https://doi.org/10.1007/s41365-018-0452-7
7. D. Kharzeev, H. Satz, Charmonium interaction in nuclear matter. J. Phys. Lett. B **356**, 365–372 (1995). https://doi.org/10.1016/0370-2693(95)00798-P
8. J. Badier et al., (NA3 Collaboration), Experimental J/ψ Hadronic Production from 150-GeV/c to 280-GeV/c. J. Z. Phys. C **20**, 101 (1983). https://doi.org/10.1007/BF01573213
9. D.M. Alde et al., (E772 Collaboration), the A-dependence of J/ψ and psi-prime production at 800-GeV/c. J. Phys. Rev. Lett. **66**, 133 (1991). https://doi.org/10.1103/PhysRevLett.66.133
10. M.J. Leitch et al., (E866/NuSea Collaboration), Measurement of J/ψ and psi-prime suppression in p-A collisions at 800-GeV/c. J. Phys. Rev. Lett. **84**, 3256 (2000). https://doi.org/10.1103/PhysRevLett.84.3256
11. W.D. Lee, Ph.D. Thesis Georgia State University (1999)
12. B. Alessandro, (NA50 Collaboration), Charmonium production and nuclear absorption in p A interactions at 450-GeV. Eur. Phys. J. C **33**, 31 (2004). https://doi.org/10.1140/epjc/s2003-01539-y
13. I. Abt et al., (HERA-B Collaboration), Kinematic distributions and nuclear effects of J/ψ production in 920-GeV fixed-target proton-nucleus collisions. Eur. Phys. J. C **60**, 525 (2009). https://doi.org/10.1140/epjc/s10052-009-0965-7
14. B. Abelev, et al., (ALICE Collaboration), J/ψ production and nuclear effects in p-Pb collisions at $\sqrt{S_{NN}} = 5.02$ TeV. J. JHEP **1402**, 073 (2014). https://doi.org/10.1007/JHEP02(2014)073
15. R. Aaij et al., (LHCb Collaboration), Study of J/ψ production and cold nuclear matter effects in pPb collisions at $\sqrt{S_{NN}} = 5$ TeV. J. JHEP **1402**, 072(2014). https://doi.org/10.1007/JHEP02(2014)072
16. A. Adare et al., (PHENIX Collaboration), Cold nuclear matter effects on J/ψ yields as a function of rapidity and nuclear geometry in deuteron-gold collisions at $\sqrt{S_{NN}} = 200$ GeV. J. Phys. Rev. Lett. **107**, 142301 (2011). https://doi.org/10.1103/PhysRevLett.107.142301
17. B. Kopeliovich, Nuclear suppression of J/ψ: from RHIC to the LHC. J. Nucl. Phys. A **864**, 203 (2011). https://doi.org/10.1016/j.nuclphysa.2011.06.024
18. E. Ferreiro, Centrality, rapidity, and transverse-momentum dependence of gluon shadowing and antishadowing on J/ψ production in d-Au collisions at $\sqrt{S_{NN}} = 200$ GeV. J. Few Body Syst. **53**, 27 (2012). https://doi.org/10.1007/s00601-012-0310-9
19. F. Arleo, Heavy-quarkonium suppression in p-A collisions from parton energy loss in cold QCD matter. J. JHEP **1303**, 122 (2013). https://doi.org/10.1007/JHEP03(2013)122
20. L.H. Song, C.G. Duan, J/ψ suppression in p-A collisions from charm quarks energy loss in cold nuclear matter. J. Phys. G **43**, 025101 (2016). https://doi.org/10.1088/0954-3899/43/2/025101
21. L.H. Song, Energy loss of charm quarks from J/ψ production in cold nuclear matter. J. Chin. Phys. C **38**, 124103 (2014). https://doi.org/10.1088/1674-1137/38/12/124103
22. C.J. Benesh, J/ψ suppression in hadron-nucleus collisions. J. Phys. Rev. C **50**, 1015 (1994). https://doi.org/10.1103/PhysRevC.50.1015
23. C.A. Salgado, U.A. Wiedemann, Calculating quenching weights. J. Phys. Rev. D **68**, 014008 (2003). https://doi.org/10.1103/PhysRevD.68.014008
24. C.A. Salgado, U.A. Wiedemann, A dynamical scaling law for jet tomography. Phys. Rev. Lett. **89**, 092303 (2002). https://doi.org/10.1103/PhysRevLett.89.092303

25. H. Fritzsch, Producing heavy quark flavors in hadronic collisions: a test of quantum chromodynamics. J. Phys. Lett. B **67**, 217 (1977). https://doi.org/10.1016/0370-2693(77)90108-3
26. M. Kramer, Quarkonium production at high-energy collidersprog. J. Part. Nucl. Phys. **47**, 141 (2001). https://doi.org/10.1016/S0146-6410(01)00154-5
27. I. Abt, Angular distributions of leptons from J/ψ's produced in 920 GeV fixed-target proton-nucleus collisions.J. Eur. Phys. J. C **60**, 517 (2009). https://doi.org/10.1140/epjc/s10052-009-0957-7
28. I. Abt, A measurement of the ψ ' to J/ψ production ratio in 920-GeV proton–nucleus interactions. Eur. Phys. J. C **49**, 545 (2007). https://doi.org/10.1140/epjc/s10052-006-0139-9
29. T.H. Chang, J/ψ polarization in 800-GeV p-Cu interactions. J. Phys. Rev. Lett. **91**, 211801 (2003). https://doi.org/10.1103/PhysRevLett.91.211801
30. R. Gavai, Quarkonium production in hadronic collisions. Int. J. Mod. Phys. A **10**, 3043 (1995). https://doi.org/10.1142/S0217751X95001443
31. G.T. Bodwin, Comparison of the color-evaporation model and the NRQCD factorization approach in charmonium production. J. Phys. Rev. D **72**, 014004 (2005). https://doi.org/10.1103/PhysRevD.72.014004
32. J. Babcock, QCD estimates for heavy particle production. J. Phys. Rev. D **18**, 162 (1978). https://doi.org/10.1103/PhysRevD.18.162
33. http://www.aip.org/pubservs/epaps.html
34. N. Liu, Nuclear geometry effect and transport coefficient in semi-inclusive lepton-production of hadrons off nuclei. J. Phys. Lett. B **749**, 88 (2015). https://doi.org/10.1016/j.physletb.2015.07.048
35. A. Accardi, Talk at from RHIC to LHC: Achievements and Opportunities (INT, Seattle, 2006)
36. A. Accardi, Space-time evolution of hadronization. Eur. Phys. J. C **49**, 347 (2007). https://doi.org/10.1140/epjc/s10052-006-0055-z
37. A. Accardi, Can we distinguish energy loss from hadron absoprtion. J. Acta Phys. Hung. A **27**, 189 (2006). https://doi.org/10.1556/APH.27.2006.2-3.2
38. C.-G. Duan, X. Jian-Chao, L.-H. Song, Nuclear effects on J/ψ production in proton–nucleus collisions. Eur. Phys. J. C **67**, 173–179 (2010). https://doi.org/10.1140/epjc/s10052-010-1270-1
39. R.J. Glauber, G. Matthiae, High-energy scattering of protons by nuclei. J. Nucl. Phys. B **21**, 135 (1970). https://doi.org/10.1016/0550-3213(70)90511-0
40. C.Y. Wong, Initial energy density of quark gluon plasma in relativistic heavy ion collisions. J. Phys. Rev. D **30**, 961 (1984). https://doi.org/10.1103/PhysRevD.30.961
41. D. Kharzeev, H. Satz, Colour confinement in hadron-nucleus collisions. J. Z. Phys. C **60**, 389 (1993)
42. F. James, CERN Program Library Long Writeup D506
43. K.J. Eskola, EPS09: a new generation of NLO and LO nuclear parton distribution functions. J. JHEP **0904**, 065 (2009). https://doi.org/10.1088/1126-6708/2009/04/065
44. J. Pumplin, New generation of parton distributions with uncertainties from global QCD analysis. J. JHEP **0207**, 012 (2002). https://doi.org/10.1088/1126-6708/2002/07/012
45. C.G. Duan, Energy loss effect in high energy nuclear Drell–Yan process. Eur. Phys. J. C **29**, 557 (2003). https://doi.org/10.1140/epjc/s2003-01256-7
46. L.H. Song, L.W. Yan, Constraining the transport coefficient in cold nuclear matter with the Drell–Yan process. J. Phys. Rev. C **96**, 045203 (2017). https://doi.org/10.1103/PhysRevC.96.045203
47. N. Armesto, Medium-induced gluon radiation off massive quarks fills the dead cone. Phys. Rev. D **69**, 114003 (2004). https://doi.org/10.1103/PhysRevD.69.114003
48. Y.L. Dokshitzer, D.E. Kharzeev, Heavy quark colorimetry of QCD matter. Phys. Lett. B **519**, 199–206 (2001). https://doi.org/10.1016/S0370-2693(01)01130-3
49. K.J. Eskola et al., EPPS16: nuclear parton distributions with LHC data. Eur. Phys. J. C **77**, 163 (2017). https://doi.org/10.1140/epjc/s10052-017-4725-9